All-Optical Storage of Phase-Sensitive Quantum States of Light

Yosuke Hashimoto,[1] Takeshi Toyama,[1] Jun-ichi Yoshikawa,[1,*] Kenzo Makino,[1] Fumiya Okamoto,[1] Rei Sakakibara,[1] Shuntaro Takeda,[1,3] Peter van Loock,[2] and Akira Furusawa[1,†]

[1]*Department of Applied Physics, School of Engineering, The University of Tokyo, 7-3-1 Hongo, Bunkyo-ku, Tokyo 113-8656, Japan*
[2]*Institute of Physics, Johannes Gutenberg-Universität Mainz, Staudingerweg 7, 55099 Mainz, Germany*
[3]*Institute of Engineering Innovation, School of Engineering, The University of Tokyo, 2-11-16 Yayoi, Bunkyo-ku, Tokyo 113-8656, Japan*

(Received 24 October 2018; published 12 September 2019)

We experimentally demonstrate storage and on-demand release of phase-sensitive, photon-number superposition states of the form $\alpha|0\rangle + \beta e^{i\theta}|1\rangle$ for an optical quantized oscillator mode. For this purpose, we newly developed a phase-probing mechanism compatible with a storage system composed of two concatenated optical cavities, which was previously employed for storage of phase-insensitive single-photon states [Phys. Rev. X **3**, 041028 (2013)]. This is the first demonstration of all-optically storing highly nonclassical and phase-sensitive quantum states of light. The strong nonclassicality of the states after storage becomes manifest as a negative region in the corresponding Wigner function shifted away from the origin in phase space. This negativity is otherwise, without the phase information of the memory system, unobtainable. While our scheme includes the possibility of optical storage, on-demand release and synchronization of arbitrary single-rail qubit states, it is not limited to such states. In fact, our technique is extendible to more general phase-sensitive states such as multiphoton superposition or entangled states, and thus it represents a significant step toward advanced optical quantum information processing, where highly nonclassical states are utilized as resources.

DOI: 10.1103/PhysRevLett.123.113603

Optical quantum states are indispensable as flying quantum information carriers, and furthermore, they can serve as sufficient resources for universal and fault-tolerant quantum computing. Prominent examples of photonic quantum information processing are the Knill-Laflamme-Milburn scheme [1], based on discrete variables and photon detections, and the Gottesman-Kitaev-Preskill scheme [2,3], based on continuous variables and homodyne detections. In these applications, the on-demand release of optical states from quantum memories is necessary. More specifically, a frequently executed process like gate teleportation [4,5], by which a probabilistically induced nonlinearity can be efficiently incorporated into a quantum protocol [6], relies, to a certain extent, on an on-demand release from quantum memories in order to synchronize the probabilistically generated auxiliary resource states.

Even though many experiments with quantum memories have been performed for a couple of decades [7], only recently were optical single-photon states with high purity, having a negative region in the Wigner function, stored and released on demand [8,9]. Storage of highly pure single-photon states was demonstrated there with two different memory systems, one based on concatenated cavities [8] and the other based on atomic ensembles [9]. The cavity systems were then used for synchronization of two photons showing Hong-Ou-Mandel interference [10].

The above high-purity memories are, in principle, capable of storing arbitrary quantum states of a harmonic oscillator $\sum_{n=0}^{\infty} c_n|n\rangle$, where photon-number eigenstates $|n\rangle$ form an orthonormal basis. However, for the successful demonstration of such a universal quantum memory, one technical challenge has remained: the phase synchronization between the internal memory fields and the external fields to be exploited via subsequent processors or measurement devices. For this purpose, phase-probing beams must be coupled to the complicated memory system, effectively having a narrow linewidth, in a stable fashion. Fock states $|n\rangle$, including a single-photon state $|1\rangle$, and their incoherent mixtures, are phase-insensitive states and thus highly pure single-photon states were stored already in previous demonstrations without tracking the optical phase inside the memory. However, many important resource states are coherent superpositions of Fock states, such as cubic phase states (i.e., the ancillae for the Gottesman-Kitaev-Preskill scheme), superpositions of coherent states [11], and entangled states in the case of two or more modes. Therefore, the introduction of a phase reference to the memory system is crucial.

In this Letter, we demonstrate storage and controlled release of general phase-sensitive superpositions of vacuum and one-photon states $c_0|0\rangle + c_1|1\rangle$ $(c_0,\ c_1 \in \mathbb{C})$ for a single optical mode, i.e., an, in principle, arbitrary single-rail qubit. We introduce coherent beams as a phase

reference to the concatenated cavity system [8,10], by which the memory-cavity frequency is further stabilized and also the optical phases of the external systems are locked. As a result, we demonstrate for the first time all-optical storage of phase-sensitive quantum states with a negative region of the Wigner function shifted from the origin in phase space. This negative region originates from the off-diagonal elements $|0\rangle\langle 1|$, $|1\rangle\langle 0|$ of the density matrix and it is strictly no longer obtainable without phase synchronization between the memory and external systems. The negative region is preserved for a storage time of up to about 200 ns, but the genuine non-Gaussianity (any non-Gaussian features indescribable by incoherently mixing Gaussian states) is kept for even longer, namely for about 400 ns [12]. Beyond storage of arbitrary single-rail (single-mode) qubits, even more importantly, our phase-preserving memory scheme is further applicable to arbitrary optical quantum states $|\psi\rangle = \sum_n c_n|n\rangle$, and paves the way for the synchronization of phase-sensitive states, which is fundamentally important for both optical quantum computing [19,20] and quantum communication [21].

The creation of highly pure non-Gaussian states typically requires strong nonlinearities, which is still difficult to obtain deterministically at present. Therefore, we resort to probabilistic schemes, where photon detections herald successful events. We start from two-mode squeezed vacuum states $|\Psi\rangle \propto \sum_{n\geq 0}(\tanh\gamma)^n|n\rangle_s|n\rangle_i$ obtained by parametric down-conversion, where signal (s) and idler (i) fields are entangled. Then we perform measurements on the idler field. If the idler field is subject to a photon counter and the measurement outcome is one photon, the signal field is projected onto a single-photon state. A more general measurement on the idler field, introducing auxiliary coherent beams, in principle enables one to project the signal field onto arbitrary states of a single mode [13,14], as well as certain classes of multimode states [22]. However, the times of successful events in the heralding scheme are random. Memory systems are powerful, because they give timing controllability to probabilistically prepared states.

The concept of our memory system to store and release general superposition states is shown in Fig. 1. Parametric down-conversion occurs inside a memory cavity, where the signal and idler fields are separated in frequency by the free spectral range of the memory cavity [8]. The shutter at the output of the memory is actually another cavity, which can transmit either the signal or the idler via the resonance condition. Initially, the shutter cavity transmits the idler field, whereas the signal field is not transmitted. By performing general measurements on the emerging idler field, the signal field inside the memory cavity is projected onto various states. Whenever the created signal state should be available for further processing and exploitation, it can be released at a controlled timing by shifting the resonance of the shutter cavity. The resonance shift is done

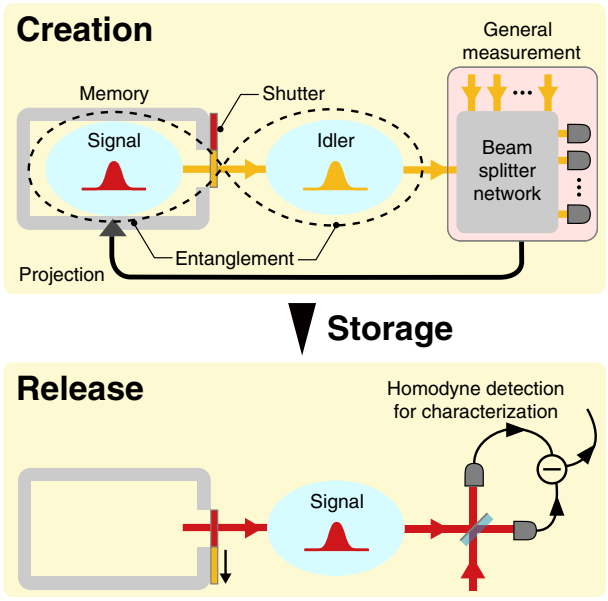

FIG. 1. Conceptual diagram of creation, storage, and on-demand release of phase-sensitive quantum states. The memory and shutter are implemented by concatenated cavities.

by utilizing an electro-optic modulator (EOM) contained inside the shutter cavity.

Figure 2 shows our experimental setup. It is based on a previous, phase-untrackable system employed for storage of single-photon states [8,10]. In order to add an optical phase reference to the memory system, we inject coherent beams that we refer to as probe beams into the memory cavity for both the signal and idler fields. The probe beams are utilized as follows. First, the memory-cavity resonance frequency is further stabilized by using the cavity transmission fringe of the signal probe beam. Next, the relative phase among the signal and idler probe beams and the pump beam is locked by monitoring their phase-sensitive parametric amplification. Finally, the transmitted probe beams are employed for feedback control of the optical phases outside the concatenated cavities. This includes the auxiliary coherent beam that is combined with the idler field to create superpositions and a local oscillator (LO) beam at the signal frequency for homodyne characterization. However, these probe beams should not be present when superposition states are created, because they destroy the heralding and homodyne signals. Therefore, the probe beams are periodically chopped by using acousto-optic modulators (AOMs), and the superposition states are created when the probe beams are absent. We switch the system between the feedback-control phase and the state-creation phase with a period of 200 ms, during which 50 ms are utilized for the state creation. The duty cycle is smaller than that of the previous experiments without the probe beams [8,10], because we have to wait for the decay of the probe beams inside the memory cavity.

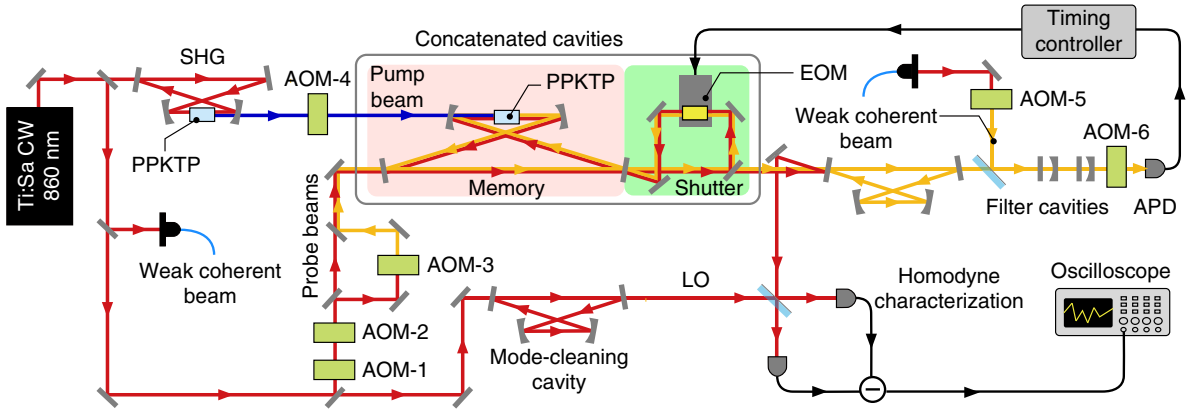

FIG. 2. Experimental setup. The light source is a continuous-wave (cw) Ti:sapphire laser operating at 860 nm. Optical frequencies of beams are distinguished by colors: Red (gray), orange (light gray), and blue (dark gray) stand for signal, idler, and pump frequencies, respectively, while small detuning is not indicated by colors. Black lines stand for electronic signal lines. Here, SHG denotes a second harmonic generator, PPKTP a periodically poled $KTiOPO_4$ crystal.

The auxiliary coherent beam at the idler frequency determines the created superposition state $\alpha|0\rangle + \beta e^{i\theta}|1\rangle$. The amplitudes α and β as well as the phase θ are independently adjustable by changing the amplitude and the phase of the auxiliary coherent beam [13–15]. An avalanche photodiode (APD) heralds the superposition state, and after a predetermined storage time controlled by a field-programmable gate array, the signal state is released. A typical photon-detection rate for creation of $(|0\rangle + e^{i\theta}|1\rangle)/\sqrt{2}$ is about 1500 counts per second, among which fake clicks caused by stray light are estimated to be about 50 counts per second. For simplicity, some beams for controlling the optical systems are omitted from the figure. More details of the methods are given in the Supplemental Material (SM) [12].

One thing to note here is that the resonance frequency of the memory cavity is detuned by about 300 kHz from the frequency of the LO for homodyne characterization. This detuning is for the purpose of avoiding unexpected photons stored by the memory, which originate from scattering of the LO (probably backscattering at the photodiodes of the homodyne detector). Such a scattering rate is very low, but we emphasize that even scattered light at the single-photon level disturbs the experiment if it couples to the memory cavity. Thanks to the detuning, the effects of the LO scattering are almost entirely removed. The signal states characterized by the homodyne detection are in a rotational frame and evolve temporally at an angular velocity of about $2\pi \times 300$ kHz. This will be seen later in the experimental results as phase shifts of the quantum state during storage. In order to achieve such an effective detuning, the signal probe beam is actually detuned by 200 kHz from the LO. Details on this technique can be found in the SM [12]. We also note that this detuning is not necessary if we could use a sufficiently good optical isolator, by which the scattered LO is removed [23].

We first show the phase-sensitive quadrature distribution of $(|0\rangle + e^{i\theta}|1\rangle)/\sqrt{2}$ obtained by the homodyne detection in Fig. 3. Figure 3(a) shows the experimental quadrature distribution with immediate release after heralding, while Fig. 3(b) shows the theoretical distribution with an ideal pure state $(|0\rangle + |1\rangle)/\sqrt{2}$. The experimental quadrature distribution is obtained by repeating the sequence of storage and release 5000 times at each of the measurement phases from 0° to 350° at an interval of 10°. The horizontal axis corresponds to the measurement phase, while the vertical axis corresponds to the quadrature value obtained from the homodyne signal. The experimental distribution

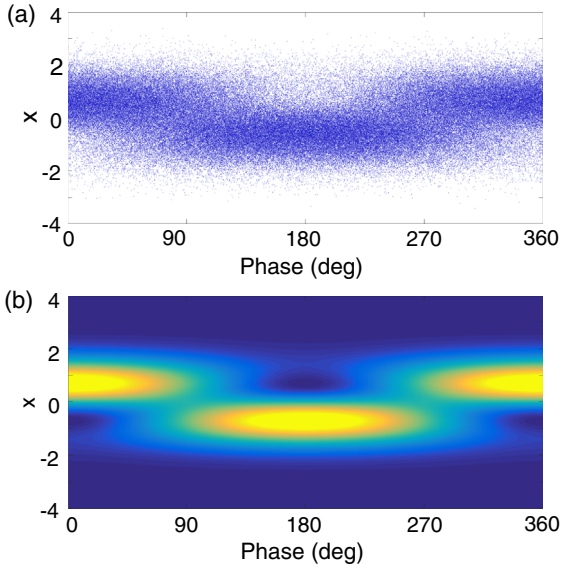

FIG. 3. Quadrature distributions of $(|0\rangle + |1\rangle)/\sqrt{2}$ for various measurement phases. (a) Experimental quadrature distribution obtained by homodyne measurements, when the created states are immediately released. (b) Theoretical quadrature distribution for the ideal pure state.

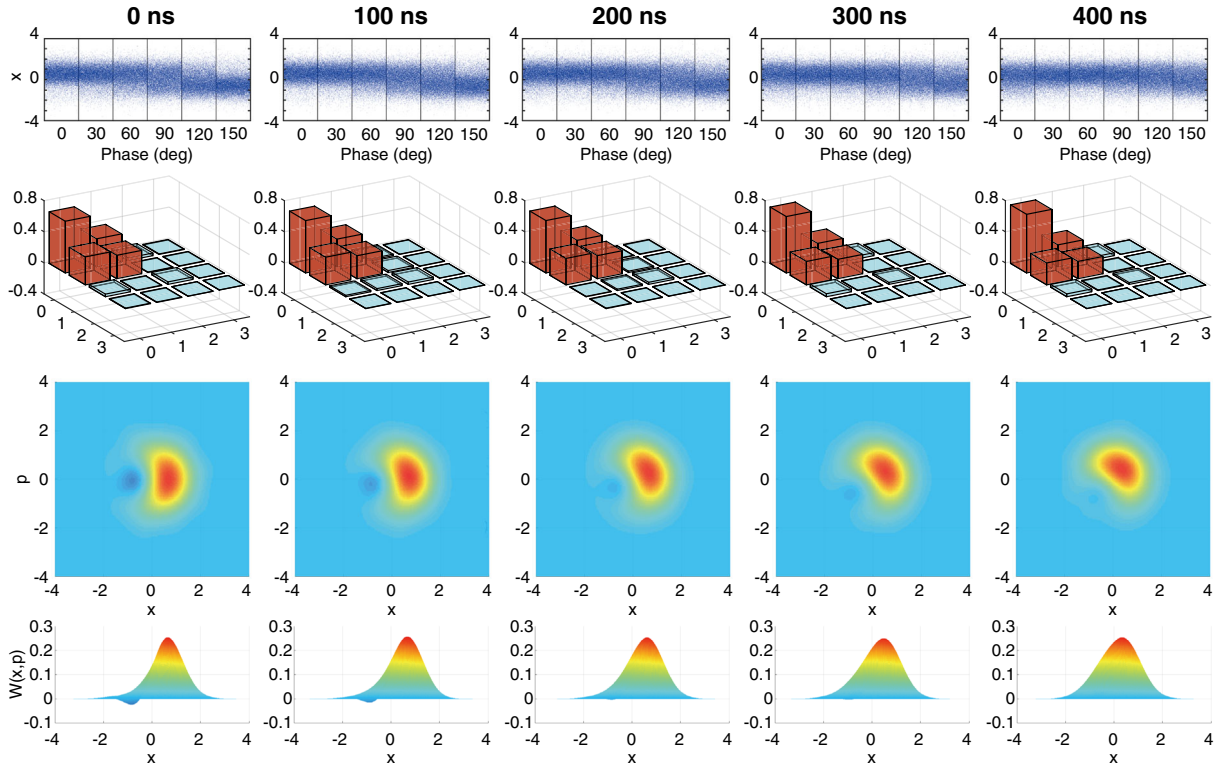

FIG. 4. Experimental results of storing $(|0\rangle + |1\rangle)/\sqrt{2}$ with various storage time. From left to right, the storage time varies from 0 to 400 ns in steps of 100 ns. First row: quadrature distributions obtained by homodyne measurements. Second row: absolute values of reconstructed density matrix elements. Red elements represent the subspace spanned by $|0\rangle$ and $|1\rangle$, and light blue elements represent the multiphoton components. Third row: Wigner functions $W(x, p)$ with $\hbar = 1$ seen from the top, corresponding to the reconstructed density matrices. Fourth row: Wigner functions $W(x, p)$ seen from the side. Minimum values are $W(-0.84, 0.09) = -0.024$ in 0 ns, $W(-0.88, -0.23) = -0.015$ in 100 ns, and $W(-0.84, -0.37) = -0.004$ in 200 ns, where statistical errors of the Wigner values are estimated as ± 0.001.

shows the phase-sensitive nature of the quantum states similar to the theoretically predicted distribution. This distribution contains sufficient information to reconstruct the density matrix and the Wigner function [24].

Next, we implemented various storage times for $(|0\rangle + |1\rangle)/\sqrt{2}$ estimating the released quantum state for each case. The experimental results are shown in Fig. 4. The storage times are 0, 100, 200, 300, and 400 ns from left to right.

The first row shows the quadrature distributions, where measurement phases are 0°, 30°, 60°, 90°, 120°, and 150°, and the number of points is 20 000 for each measurement phase. Even for the case of 400 ns storage time, the phase-sensitive nature of the memorized states clearly remains. The distribution shifts horizontally depending on the storage time, which is explained by the 300 kHz detuning explained above. From the quadrature distributions, the density matrices and the Wigner functions are estimated.

The second row shows the reconstructed density matrices, where the absolute value is taken for each matrix element. The matrix elements of the subspace up to one photon are colored in red (gray). Multiphoton components, colored in light blue (light gray), are very small (less than 5%). We can see that the off-diagonal elements are nicely preserved during the storage, though some portion of the single-photon component $|1\rangle\langle 1|$ is converted to a vacuum component $|0\rangle\langle 0|$ mainly due to intracavity losses (about 0.2% for each round-trip of 1.5 m). The phase shifts of the off-diagonal elements due to the detuning are not visible, because the absolute value is taken for each element. In the SM, real and imaginary parts of the density matrices are separately plotted, so that one can see the phase shifts during storage [12]. We also discuss in the SM the amount of phase fluctuations estimated from the density matrices [12]. In the analysis, we divide imperfections into optical losses and phase fluctuations, which leads to estimated fluctuations from 20° to 35°. We did not find a clear tendency towards worse dephasing during storage.

The third and fourth rows are the Wigner functions seen from the top and the side. Seen from the top, the state rotates with an angle proportional to the storage time. Again, this rotation corresponds to the 300 kHz detuning mentioned above. Seen from the side, the negative region of Wigner function clearly remains with a storage time of

100 ns, and it is still visible with a storage time of 200 ns. The negative region is not at the origin, unlike for the previous single-photon case [8], and therefore this negativity exhibits nonclassicality that cannot be preserved without the phase information of the quantum state. Moreover, even with longer storage times where the negativity is lost, the Wigner function still satisfies a criterion of genuine non-Gaussianity (i.e., the distribution cannot be produced by a classical mixture of Gaussian states) [16], which we discuss in more detail in the SM [12].

We also confirmed that the parameters α, β, θ of the superposition $\alpha|0\rangle + \beta e^{i\theta}|1\rangle$ are controllable in the state-preparation stage. Experimental results with other states, such as $(|0\rangle - i|1\rangle)/\sqrt{2}$ and $(|0\rangle + \sqrt{2}|1\rangle)/\sqrt{3}$, are shown in the SM [12] and these are consistent with the above results.

In conclusion, we experimentally demonstrated creation, storage, and on-demand release of phase-sensitive optical quantum states like $\alpha|0\rangle + \beta e^{i\theta}|1\rangle$ by employing a concatenated cavity system. We succeeded in storing quantum states with a negative region in the Wigner function shifted away from the phase-space origin—a feature only possible with a phase-trackable memory system. Generally, the phase-tracking mechanism is very important for a memory system, because many quantum features such as quantum entanglement are lost without the phase information. Our demonstration paves the way for future demonstrations of storing various quantum states such as Schrödinger cat states, cubic phase states, and so forth. The event rate will increase if we use superconductive single-photon detectors [25] or photon-number resolving detectors with transition-edge sensor [26], which have higher quantum efficiencies.

This work was partly supported by JSPS KAKENHI (Grants No. 18H01149 and No. 18H05207), CREST (Grant No. JPMJCR15N5) of JST, the UTokyo Foundation, and donations from Nichia, of Japan. Y. H. acknowledges support from ALPS. P. v. L. acknowledges support from Q.Link.X (BMBF) in Germany.

*yoshikawa@ap.t.u-tokyo.ac.jp
†akiraf@ap.t.u-tokyo.ac.jp

[1] E. Knill, R. Laflamme, and G. Millburn, A scheme for efficient quantum computation with linear optics, Nature (London) **409**, 46 (2001).
[2] D. Gottesman, A. Kitaev, and J. Preskill, Encoding a qubit in an oscillator, Phys. Rev. A **64**, 012310 (2001).
[3] K. Fukui, A. Tomita, and A. Okamoto, Analog Quantum Error Correction with Encoding a Qubit into an Oscillator, Phys. Rev. Lett. **119**, 180507 (2017).
[4] D. Gottesman and I. L. Chuang, Demonstrating the viability of universal quantum computation using teleportation and single-qubit operations, Nature (London) **402**, 390 (1999).
[5] S. D. Bartlett and W. J. Munro, Quantum Teleportation of Optical Quantum Gates, Phys. Rev. Lett. **90**, 117901 (2003).
[6] K. Miyata, H. Ogawa, P. Marek, R. Filip, H. Yonezawa, J. Yoshikawa, and A. Furusawa, Implementation of a quantum cubic gate by an adaptive non-Gaussian measurement, Phys. Rev. A **93**, 022301 (2016).
[7] A. I. Lvovsky, B. C. Sanders, and W. Tittel, Optical quantum memory, Nat. Photonics **3**, 706 (2009).
[8] J. Yoshikawa, K. Makino, S. Kurata, P. van Loock, and A. Furusawa, Creation, Storage, and On-Demand Release of Optical Quantum States with a Negative Wigner Function, Phys. Rev. X **3**, 041028 (2013).
[9] E. Bimbard, R. Boddeda, N. Vitrant, A. Grankin, V. Parigi, J. Stanojevic, A. Ourjoumtsev, and P. Grangier, Homodyne Tomography of a Single Photon Retrieved on Demand from a Cavity-Enhanced Cold Atom Memory, Phys. Rev. Lett. **112**, 033601 (2014).
[10] K. Makino, Y. Hashimoto, J. Yoshikawa, H. Ohdan, T. Toyama, P. van Loock, and A. Furusawa, Synchronization of optical photons for quantum information processing, Sci. Adv. **2**, e1501772 (2016).
[11] T. C. Ralph, A. Gilchrist, G. J. Milburn, W. J. Munro, and S. Glancy, Quantum computation with optical coherent states, Phys. Rev. A **68**, 042319 (2003).
[12] See Supplemental Material at http://link.aps.org/supplemental/10.1103/PhysRevLett.123.113603 for the methods, experimental results with various coefficients, analysis of non-Gaussianity, and analysis of phase fluctuations, which includes Refs. [8,10,13–18].
[13] E. Bimbard, N. Jain, A. MacRae, and A. I. Lvovsky, Quantum-optical state engineering up to the two-photon level, Nat. Photonics **4**, 243 (2010).
[14] M. Yukawa, K. Miyata, T. Mizuta, H. Yonezawa, P. Marek, R. Filip, and A. Furusawa, Generating superposition of up-to three photons for continuous variable quantum information processing, Opt. Express **21**, 5529 (2013).
[15] J. S. Neergaard-Nielsen, M. Takeuchi, K. Wakui, H. Takahashi, K. Hayasaka, M. Takeoka, and M. Sasaki, Optical Continuous-Variable Qubit, Phys. Rev. Lett. **105**, 053602 (2010).
[16] M. G. Genoni, M. L. Palma, T. Tufarelli, S. Olivares, M. S. Kim, and M. G. A.Paris, Detecting quantum non-Gaussianity via the Wigner function, Phys. Rev. A **87**, 062104 (2013).
[17] A. MacRae, T. Brannan, R. Achal, and A. I. Lvovsky, Tomography of a High-Purity Narrowband Photon from a Transient Atomic Collective Excitation, Phys. Rev. Lett. **109**, 033601 (2012).
[18] O. Morin, C. Fabre, and J. Laurat, Experimentally Accessing the Optimal Temporal Mode of Traveling Quantum Light States, Phys. Rev. Lett. **111**, 213602 (2013).
[19] S. Takeda, T. Mizuta, M. Fuwa, P. van Loock, and A. Furusawa, Deterministic quantum teleportation of photonic quantum bits by a hybrid technique, Nature (London) **500**, 315 (2013).
[20] S. Takeda and A. Furusawa, Universal Quantum Computing with Measurement-Induced Continuous-Variable Gate Sequence in a Loop-Based Architecture, Phys. Rev. Lett. **119**, 120504 (2017).

[21] L.-M. Duan, M. D. Lukin, J. I. Cirac, and P. Zoller, Long-distance quantum communication with atomic ensembles and linear optics, Nature (London) **414**, 413 (2001).

[22] J. Yoshikawa, M. Bergmann, P. van Loock, M. Fuwa, M. Okada, K. Takase, T. Toyama, K. Makino, S. Takeda, and A. Furusawa, Heralded creation of photonic qudits from parametric down-conversion using linear optics, Phys. Rev. A **97**, 053814 (2018).

[23] O. Morin, V. D'Auria, C. Fabre, and J. Laurat, High-fidelity single-photon source based on a Type II optical parametric oscillator, Opt. Lett. **37**, 3738 (2012).

[24] A. Lvovsky, Iterative maximum-likelihood reconstruction in quantum homodyne tomography, J. Opt. B **6**, S556 (2004).

[25] H. Le Jeannic, V. B. Verma, A. Cavaillès, F. Marsili, M. D. Shaw, K. Huang, O. Morin, S. W. Nam, and J. Laurat, High-efficiency WSi superconducting nanowire single-photon detectors for quantum state engineering in the near infrared, Opt. Lett. **41**, 5341 (2016).

[26] D. Fukuda, G. Fujii, T. Numata, K. Amemiya, A. Yoshizawa, H. Tsuchida, H. Fujino, H. Ishii, T. Itatani, S. Inoue, and T. Zama, Titanium-based transition-edge photon number resolving detector with 98% detection efficiency with index-matched small-gap fiber coupling, Opt. Express **19**, 870 (2011).